

1 **Search for High Ionizing Particles in 8 TeV**
2 ***pp* Collisions at the LHC Using the Full LHC Run-1 MoEDAL Detector**

3 B. Acharya,^{1,*} J. Alexandre,¹ P. Benes,² B. Bergmann,² J. Bernabéu,³ A. Bevan,⁴ H. Branzas,⁵ P. Burian,²
4 M. Campbell,⁶ S. Cecchini,⁷ Y. M. Cho,⁸ M. de Montigny,⁹ A. De Roeck,⁶ J. R. Ellis,^{1,10,†} M. El Sawy,^{6,‡}
5 M. Fairbairn,¹ D. Felea,⁵ M. Frank,¹¹ J. Hays,⁴ A. M. Hirt,¹² J. Janecek,² M. Kalliokoski,¹³ A. Korzenev,¹⁴
6 D. H. Lacarrère,⁶ C. Leroy,¹⁵ G. Levi,¹⁶ P. Li,⁹ A. Lioni,¹⁴ J. Mamuzic,³ A. Maulik,^{7,9} A. Margiotta,¹⁶ N. Mauri,⁷
7 N. E. Mavromatos,¹ P. Mermod,^{14,§} M. Mieskolainen,¹³ L. Millward,⁴ V. A. Mitsou,³ R. Orava,¹³ I. Ostrovskiy,¹⁷
8 P.-P. Ouimet,^{9,¶} J. Papavassiliou,³ B. Parker,¹⁸ L. Patrizii,⁷ G. E. Pāvāļas,⁵ J. L. Pinfold,^{9,**} L. A. Popa,⁵
9 V. Popa,⁵ M. Pozzato,⁷ S. Pospisil,² A. Rajantie,¹⁹ R. Ruiz de Austri,³ Z. Sahnoun,^{7,††} M. Sakellariadou,¹
10 A. Santra,³ S. Sarkar,¹ G. Semenoff,²⁰ A. Shaa,⁹ G. Sirri,⁷ K. Sliwa,²¹ R. Soluk,⁹ M. Spurio,¹⁶ M. Staelens,⁹
11 M. Suk,² M. Tenti,²² V. Togo,⁷ J. A. Tuszyński,⁹ A. Upreti,¹⁷ V. Vento,³ O. Vives,³ and A. Wall¹⁷

12 (THE MoEDAL COLLABORATION)

13 ¹*Theoretical Particle Physics & Cosmology Group, Physics Dept., King's College London, UK*

14 ²*IEAP, Czech Technical University in Prague, Czech Republic*

15 ³*IFIC, Universitat de València - CSIC, Valencia, Spain*

16 ⁴*School of Physics and Astronomy, Queen Mary University of London, UK*

17 ⁵*Institute of Space Science, Bucharest - Măgurele, Romania*

18 ⁶*Experimental Physics Department, CERN, Geneva, Switzerland*

19 ⁷*INFN, Section of Bologna, Bologna, Italy*

20 ⁸*Center for Quantum Spacetime, Sogang University, Seoul, Korea*

21 ⁹*Physics Department, University of Alberta, Edmonton, Alberta, Canada*

22 ¹⁰*Theoretical Physics Department, CERN, Geneva, Switzerland*

23 ¹¹*Department of Physics, Concordia University, Montréal, Québec, Canada*

24 ¹²*Department of Earth Sciences, Swiss Federal Institute of Technology, Zurich, Switzerland*

25 ¹³*Physics Department, University of Helsinki, Helsinki, Finland*

26 ¹⁴*Département de Physique Nucléaire et Corpusculaire, Université de Genève, Geneva, Switzerland*

27 ¹⁵*Département de Physique, Université de Montréal, Québec, Canada*

28 ¹⁶*INFN, Section of Bologna & Department of Physics & Astronomy, University of Bologna, Italy*

29 ¹⁷*Department of Physics and Astronomy, University of Alabama, Tuscaloosa, Alabama, USA*

30 ¹⁸*Institute for Research in Schools, Canterbury, UK*

31 ¹⁹*Department of Physics, Imperial College London, UK*

32 ²⁰*Department of Physics, University of British Columbia, Vancouver, British Columbia, Canada*

33 ²¹*Department of Physics and Astronomy, Tufts University, Medford, Massachusetts, USA*

34 ²²*INFN, CNAF, Bologna, Italy*

35 (Dated: October 30, 2020)

A search for highly electrically charged objects (HECOs) and magnetic monopoles is presented using 2.2 fb^{-1} of p-p collision data taken at a centre of mass energy of 8 TeV by the MoEDAL detector during LHC's Run-1. The data were collected using MoEDAL's Nuclear Track Detector array and the Trapping Detector array. The results are interpreted in terms of Drell-Yan pair production of stable HECO and monopole pairs with three spin hypotheses (0, 1/2 and 1). The search provides constraints on the direct production of magnetic monopoles carrying one to five Dirac magnetic charges ($5g_D$) and with mass limits ranging from 710 GeV to 1230 GeV. Additionally, mass limits are placed on HECO with charge in the range $10e$ to $165e$, where e is the charge of an electron, for masses between 640 GeV and 2000 GeV.

36 PACS numbers: 14.80.Hv, 13.85.Rm, 29.20.db, 29.40.Cs

37 INTRODUCTION

38 The quest for intrinsically highly ionizing particle
39 (HIP) avatars of physics beyond the Standard Model has
40 been an active area of investigation at accelerator centres
41 for several decades [1–15]. Searches have also been per-
42 formed in cosmic rays and in matter [16, 17]. Most HIP
43 searches can be divided into two categories: the quest
44 for magnetic monopoles (MMs) and the hunt for highly
45 electrically charged objects (HECOs). According to the

46 Bethe-Bloch formula [18], massive singly charged parti-
47 cles traversing matter can also be highly ionizing due to
48 their low velocity, β (the particle velocity expressed as a
49 fraction of the speed of light, c).

50 In 1931 Dirac formulated a consistent description of a
51 magnetic monopole [19] within the framework of quan-
52 tum physics. This monopole is associated with a line of
53 singularity called a Dirac string. Dirac derived his Quan-
54 tization Condition (DQC) in order that this string has no
55 effect: $g_D = \frac{2\pi\hbar}{\mu_0 e} n$ where e is the electric charge of the

particle probe, \hbar is Planck's constant divided by 2π , g_D is the magnetic charge, μ_0 is the permeability of free space and n is an integer.

The DQC indicates that if the magnetic charge exists then the electric charge is quantized in units of $e = 2\pi\hbar/(\mu_0)g_D$. The value of g_D is approximately $68.5e$. Dirac's theory did not constrain the mass or the spin of the monopole. Further, the Dirac quantization condition indicates a coupling strength much bigger than one: $\alpha_m = \mu_0 g_D^2 / (4\pi\hbar c) \approx 34$. Thus, perturbation theory cannot be applied and cross-section calculations based on perturbation theory are not physically valid, although useful as a benchmark.

In 1974 't Hooft [20] and Polyakov [21] discovered monopole solutions of the non-Abelian Georgi-Glashow model [22]. This model has only one gauge symmetry, $SO(3)$, with a three component Higgs field. The mass of the 't Hooft–Polyakov MM was predicted to be around 100 GeV. However, MMs with such a low mass were ruled out by experiment. Subsequently, Georgi and Glashow combined their electroweak theory with a theoretical description of strong nuclear forces to form a Grand Unified Theory (GUT) [23] using the single non-Abelian gauge symmetry, $SU(5)$. In this GUT theory the MM would have a mass of $\sim 10^{15}$ GeV which is far too heavy to be directly produced at any foreseeable terrestrial collider.

Although, the Standard Model has an $SU(2) \times U(1)$ group structure that does not admit a finite-energy monopole, Cho and co-workers have modified its structure to admit the possibility of an “electroweak” monopole [24, 25] with a magnetic charge of $2g_D$. Based on this work Cho, Kim and Yoon (CKY) [26] have more recently presented an adaptation of the Standard Model, that includes a non-minimal coupling of its Higgs field to the square of its $U(1)$ gauge coupling strength, that admits the possibility of a finite energy dyon [27].

The question of whether it is possible to create generalisations of the CKY model that are consistent with the the Standard Model was considered by Ellis, Mavroumatos and You (EMY) [28]. EMY concluded that there was a possibility that an “electroweak” monopole, consistent with the current constraints on the Standard Model, may exist and be detectable at the LHC. In any case, the existence of a MM is such a theoretically well predicated and revolutionary possibility that the search for a MM has been carried out as each new energy frontier is broached.

We consider here only those models that admit a magnetic charge quantized in units of Dirac charge, g_D , or a multiple of the Dirac charge. As $g_D = 68.5e$, a relativistic monopole with a single Dirac charge will ionize ~ 4700 times more than a relativistic proton. It is thus a prime example of a HIP.

As mentioned above electrically charged HIPs, or HECOs, have also been hypothesized. Examples of HECOs, include: dyons doubly charge massive particles

[3]; aggregates of ud - [29] or s -quark matter [30], Q -balls [31], [32] and the remnants of microscopic black-holes [33].

The first searches for MMs and/or HECOs at the LHC were performed by the ATLAS and MoEDAL Collaborations in 8 TeV pp-collisions [4, 5, 8]. At this stage, the ATLAS monopole search was sensitive to singly magnetically charged ($1g_D$) monopoles, whereas the MoEDAL search was sensitive to single and multiply charged monopoles. ATLAS and MoEDAL continued the quest for HIPs at RUN2.

In the case of MMs, the ATLAS and MoEDAL searches were complementary, in the sense that ATLAS utilized the MMs highly ionizing signature [7, 14] whereas, until now, the MoEDAL experiment only exploited the induction technique to directly detect the magnetic charge [9–11]. Extensive accelerator searches for HECOs at the LHC have also been undertaken [4, 6, 7, 14]. The latest result from LHC describes the ATLAS experiment search for HECOs and monopoles using data taken during LHC's Run-2 at a centre-of-mass energy of 13 TeV [15].

In this paper we report the first use of the MoEDAL Nuclear Track Detector (NTD) System, which relies on an ionization signal to detect HIPs. The 2.2 fb^{-1} of $p-p$ collision data analyzed was obtained during LHC's Run-1 at IP8 on the LHC ring.

ENERGY LOSS OF HIPs IN MOEDAL

In the MoEDAL detector HIPs lose energy by ionization. When considering the energy loss in the MMT detector the total energy loss is computed using Bethe-Block formula. For NTDs the relevant quantity is the Restricted Energy Loss (REL) [34]. The REL is equal to the particle's total energy loss in the medium for $\beta < 10^{-2}$. At larger velocities REL is the fraction of the electronic energy loss leading to the formation of δ -rays with energies lower than a cut-off energy T_{cut} . The REL can be computed from the Bethe-Block formula restricted to energy transfers $T < T_{cut}$ with T_{cut} a constant characteristic of the medium. For Makrofol, which is the MoEDAL NTD used for the analysis reported in this paper, $T_{cut} < 350 \text{ eV}$. The RELs for MMs and for HECOs in Makrofol are shown in Fig. 1 and Fig. 2, respectively.

THE RUN-1 MOEDAL DETECTOR

During LHC's Run-1, MoEDAL deployed a prototype detector system comprised of two sub-detector systems. The first of these was a plastic Nuclear Track Detector stack array to detect the ionization trail of HIPs. The second was a detector system comprised of 163 kg of aluminium absorber elements. This detector system was

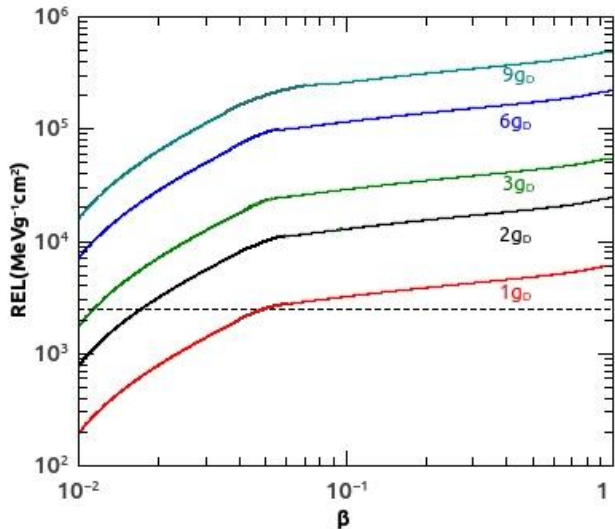


FIG. 1. Restricted Energy Loss in Makrofol for monopoles of different magnetic charge. The horizontal dotted line indicates the Makrofol detection threshold.

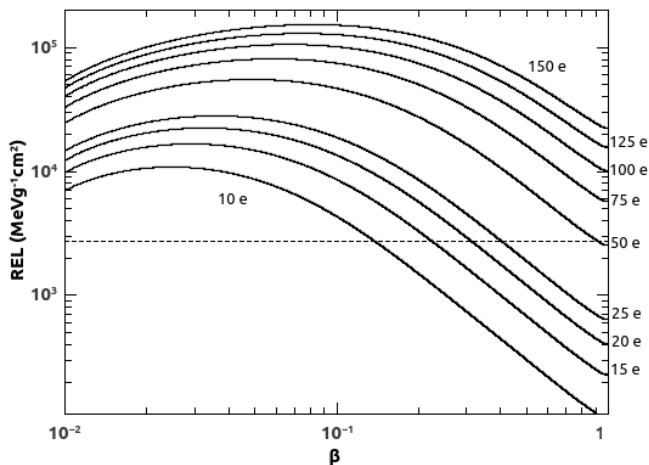


FIG. 2. Restricted Energy Loss in Makrofol for HECOs of different electric charge. The horizontal dotted line indicates the Makrofol detection threshold.

162 called the MMT (Magnetic Monopole Trapper) since it
 163 was used to trap HIPs with magnetic charge, that slow
 164 down and stop within its sensitive volume, for further
 165 laboratory analysis. Both of these detector systems were
 166 passive, requiring neither a trigger or readout electronics.
 167 The MoEDAL detector is described in more detail below.
 168

169 The MoEDAL detector is exemplified by its ability to
 170 retain a permanent record, and even capture new particles
 171 for further study. There are no Standard Model particles
 172 that can produce such distinct signatures – thus,

173 even the detection in MoEDAL of few HIP particle mes-
 174 sengers of new physics would herald a discovery.

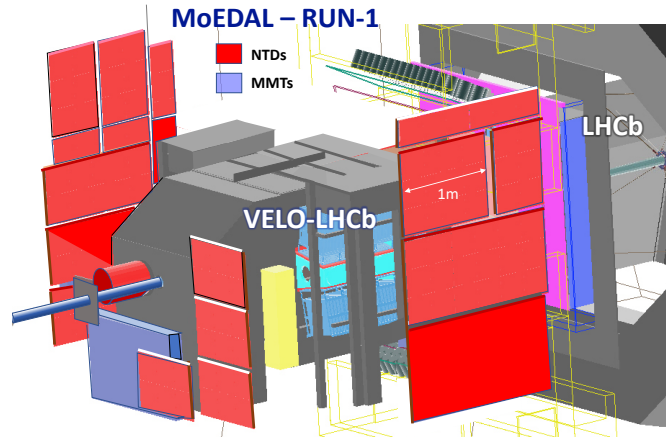


FIG. 3. The Prototype MoEDAL Detector deployed at IP8 during LHC's RUN-1.

The MMT Detector

176 The prototype MMT detector deployed for LHC's Run-
 177 1 was comprised of 198 aluminium rods weighing a total
 178 of 163 kg. These bars were housed in an enclosure
 179 placed just underneath the beampipe at the upstream
 180 end of LHCb's VELO detector as shown in Figure 3. After
 181 exposure the MMTs' Al rods are sent to the ETH Zurich
 182 Laboratory for Natural Magnetism. Here they are passed
 183 through a SQUID magnetometer to scan for the presence
 184 of trapped magnetic charge. A monopole will stop in
 185 the MMT detector when its speed falls below $\beta \leq 10^{-3}$.
 186 It then binds due to the interaction between the monopole
 187 and the nuclear magnetic moment [35–38] of an aluminium
 188 nucleus comprising in an MMT trapping volume.
 189

190 The anomalously large magnetic moment of an alu-
 191 minium nucleus gives rise to a monopole-nucleus binding
 192 energy (BE) of 0.5 - 2.5 MeV [35], comparable to the shell
 193 model splittings. In any case, it is reasonable to assume
 194 that the very strong magnetic field of the monopole will
 195 rearrange the nucleus permitting it to bind strongly to
 196 the nucleus. As reported in Ref. [35] monopoles with this
 197 BE will be bound indefinitely. It would require fields in
 198 excess of around 5T for the trapped monopole to be freed.
 199 We note that the MOEDAL experiment's MMT volumes
 200 are never subjected to such strong magnetic fields.

201

202 A magnetic monopole captured in an MMT volume
 203 is tagged and measured as a persistent current in the
 204 SQUID coil encircling the samples' transport axis that
 205 passes through the SQUID magnetometer. The cali-
 206 bration of the magnetometer response is achieved us-
 207 ing two independent techniques which are more fully re-
 208 counted in Ref. [39]. These methods agree to within 10%,
 209 which is taken to be the pole strength calibration uncer-
 210 tainty. The magnetometer response has been determined
 211 by measurement to be charge-symmetric and linear in a
 212 range of magnetic charge 0.3 - 300 g_D .

213

The Nuclear Track Detector System

214 The MoEDAL Nuclear Track Detector is organized in
 215 modules deployed around the Point-8 intersection region
 216 of the LHCb detector, in the VELO (VERTex LOcator)
 217 cavern. The NTD system, deployed for Run-2 in 2014
 218 comprises 186 modules. The results reported here refer
 219 to a prototype array of 135 modules. Each module com-
 220 prises three layers of 1.5 mm thick CR39[®] polymer, three
 221 layers of Makrofol DE[®] and three layers of Lexan[®] 0.5
 222 and 0.25 mm thick, respectively, inside Aluminium bags
 223 (Fig. 4). A sketch of the MoEDAL's prototype detector
 224 is shown in Fig. 3.

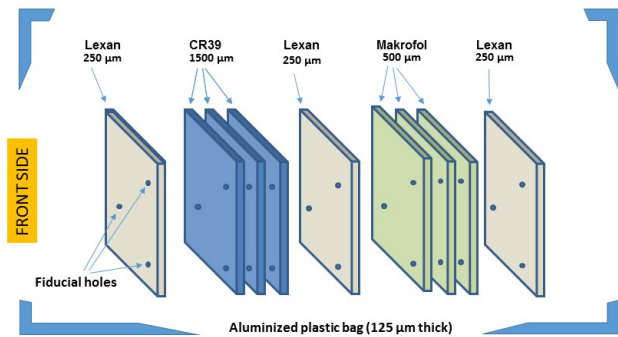


FIG. 4. NTD module composition

225

The etching procedure

226 In plastic track-etch detectors, the passage of a heav-
 227 ily ionizing particle can produce a permanent damage of
 228 polymeric bonds in a cylindrical region (“latent track”)
 229 extending few tens of nanometer around the particle tra-
 230 jectory (Fig.5). By subsequent chemical etching the bulk
 231 of the material is removed at a rate v_B and at a higher
 232 rate v_T along the latent track. The damage zone is re-
 233 vealed under an optical microscope as a cone shaped

234 etch-pit, called “track”. Etch-pits surface openings have
 235 a circular shape for normally incident particles, otherwise
 236 they are elliptical.

237 A sketch of the etch-pit at different etching times is
 238 shown in Fig.5 for a normally incident particle cross-
 239 ing the detector at a constant energy loss. Two etching
 240 conditions were applied (Table I: the so-called “strong
 241 etching” [40] allowing faster etching and yielding larger
 242 etch-pits easier to detect under visual scanning, was ap-
 243 plied to the top-most Makrofol foil in each module. “Soft
 244 etching” is a slower process allowing to proceed in several
 245 etching steps to follow the formation of etch-pits. Soft
 246 etching was applied to other Makrofol foils if a candidate
 247 track was found in the first layer.

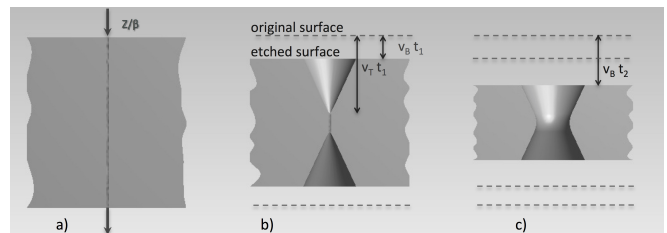


FIG. 5. Illustration of the track-etch technique: a) latent track forming along the trajectory of a high ionizing particle impinging perpendicularly on the NTD surface ; b) development of conical pits during the etching process; c) etch-pits joining after a prolonged etching, forming a hole in the detector.

248

Calibration of the NTD Detector

249 The response of the NTD is measured by the etch-
 250 ing rate ratio $p = v_T / v_B$, as a function of the particle's
 251 REL. Heavy ion beams are used to determine the detector
 252 response over a large range of energy losses, as discussed
 253 in ref. [41]. The Makrofol was calibrated with 158 A
 254 GeV Pb⁸²⁺ and 13 A GeV Xe⁵⁴⁺ ion beams at the CERN
 255 SPS. The calibration set-up included a stack of Makrofol
 256 foils placed upstream and downstream of an Aluminum
 257 target. Incoming ions undergo charge changing nuclear
 258 fragmentation along their path through the detector foils
 259 and the target. After etching the size of surface tracks
 260 was measured with an automatic scanning system pro-
 261 viding the area, and the coordinates of the center of the
 262 etch pits. The base area distributions of incoming ions
 263 and of their fragments is shown in Fig. 7. The projec-
 264 tile fragments have the same velocity and approximately
 265 the same direction as the incident ions. From the base
 266 area spectrum, the charge corresponding to each nuclear
 267 fragment peak can be identified, and the corresponding
 268 REL determined. A detailed description of the calibra-
 269 tion procedure can be found in [41].

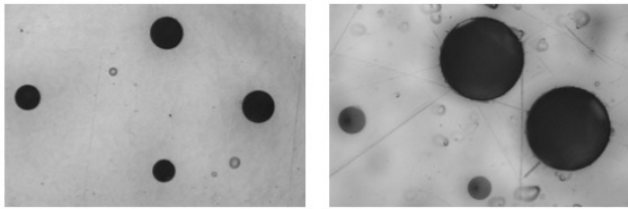


FIG. 6. Microphotographs of relativistic Pb^{82+} tracks and of nuclear fragments ($Z < 82$) in two consecutive foils of Makrofol. Etch pits are from the same ions crossing the detector foils: (left) Makrofol foil etched in “soft conditions”; (right) Makrofol foil etched in “strong conditions”.

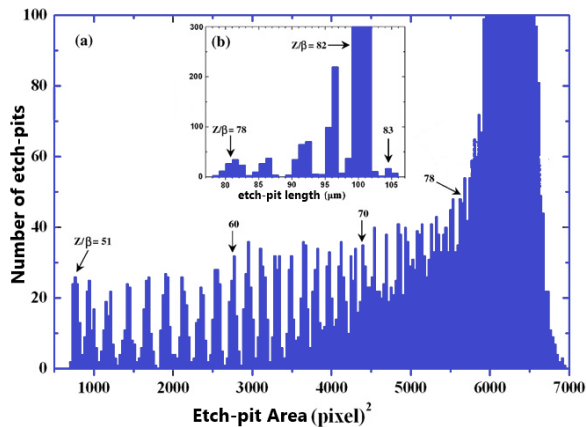


FIG. 7. Distribution of track surface areas in Makrofol exposed to 158 A GeV Pb^{82+} and etched in soft conditions [41].

270 Calibration data thus obtained are shown in Fig.8.
 271 The minimum detectable relativistic charge is $Z/\beta \geq$
 272 50, both in soft or strong etching. The detector thresh-
 273 old ($p=1$) is at $\text{REL} \sim 2700 \text{ MeV cm}^{-2} \text{g}^{-1}$.

274 *Etching and Scanning of MoEDAL NTD*

275 After exposure in the LHC IP8 region, the MoEDAL
 276 NTD stacks were brought to the INFN etching and scan-
 277 ning Lab in Bologna. A global module reference system
 278 is created by drilling three holes – 2 mm diameter – on
 279 each detector module. This coordinate system provides
 280 an accuracy of $100 \mu\text{m}$ on the determination of the po-
 281 sition of a particle track over the detector surface. The
 282 stacks are then unpacked, the detectors foils labelled and
 283 their thickness measured on a grid of points uniformly
 284 distributed over the foil surface.

285 For the search reported in this paper only Makrofol
 286 foils were analysed. In each exposed stack, the most up-
 287 stream Makrofol layer was etched in 6 N KOH + 20%
 288 Ethyl alcohol at 65°C . After 6 hours etching etch-pits as
 289 large as $10 \mu\text{m}$ would be detected under 20X magnifica-
 290 tion. An efficiency of $\sim 99\%$ was estimated by scanning

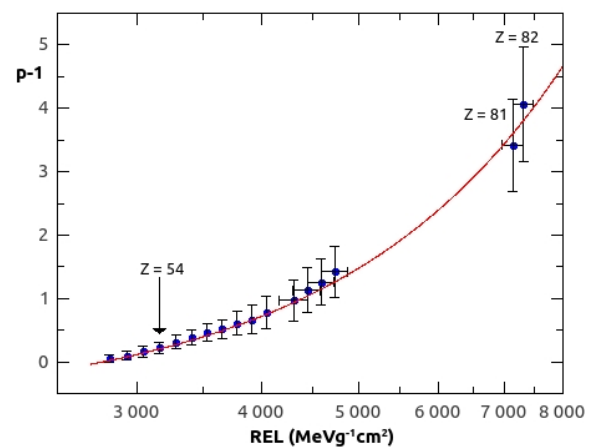
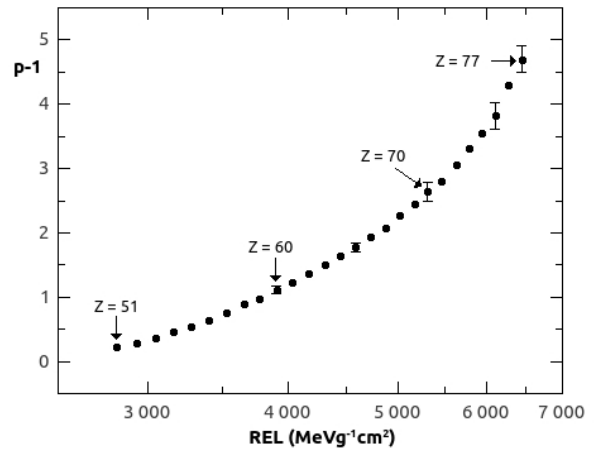


FIG. 8. Reduced etch-rate versus REL for Makrofol exposed to relativistic Lead and Xenon ion beams: (top) detectors etched in (top) soft conditions; (bottom) detectors etched in strong conditions.

291 foils exposed to ions.

292 Every detected surface structure was further observed
 293 under a larger magnification microscope and classified
 294 either as material defects or particle’s track. If a dou-
 295 ble etch-pit was detected it was observed at larger (100–
 296 200 \times) magnification. From the etch-pit size, and the
 297 bulk etching rate, the incidence angle on each surface
 298 are computed. A track was defined as a “candidate” if
 299 etch-pit sizes and incidence angles on the front and back
 300 surfaces were compatible with that of a single particle.
 301 If candidates were found in the first layer of a module,
 302 downstream Makrofol foils would be etched in 6 N KOH
 303 + 20% Ethyl alcohol at 50°C . and etch-pits’ dimensions
 304 (surface diameters, area, etch-pit length) measured in or-
 305 der to determine the particle’s direction and REL.

306 An accurate scan under an optical microscope with
 307 high magnification (100 \times) is performed in a square region
 308 of about 1 cm^2 around the candidate expected position.
 309 If a two-fold coincidence was detected, also the middle

310 layer would be etched and analyzed.

311

The Detection Threshold for Makrofol

312 For the HIP to be detected its REL must be greater
 313 than the detection threshold of the Makrofol. The detec-
 314 tion threshold will vary with the etching conditions. It
 315 will also vary with the angle of incidence of HIP on the
 316 NTD. The greater the angle of incidence the lower the de-
 317 tection threshold. The lowest threshold is obtained for a
 318 HIP impinging normally to the NTD. the curve showing
 319 the relating between angle δ_{Max} and the REL is shown
 320 in Figure 9, where δ_{Max} is the maximum angle that the
 321 HIP of a certain REL can make with the normal to the
 322 NTD plan and still be detected.

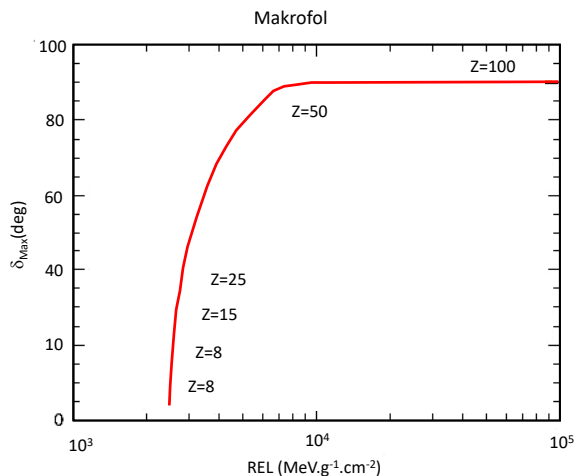


FIG. 9. The maximum angle to the normal of the NTD plane within which the HIP will be detected.

323

ACCEPTANCE OF THE RUN-1 MOEDAL DETECTOR

324

325 The MoEDAL detector's acceptance is defined to be
 326 the fraction of the number of events in which at least one
 327 HIP of the DY produced pair was detected in MoEDAL.
 328 The acceptance for Drell-Yan production of HECOs and
 329 magnetic monopoles is described by an interplay of the
 330 geometrical disposition of MoEDAL NTD modules and
 331 MMT detectors, energy loss in the detectors, mass of the
 332 particle and the spin-dependent kinematics of the inter-
 333 action products. In the case of the HECOs, MoEDAL
 334 NTD provides the only means of detection.

335 For a given HIP mass and charge, the pair-production
 336 model determines the kinematics and the overall trapping
 337 acceptance obtained. The uncertainty in the acceptance
 338 is dominated by uncertainties in the material descrip-
 339 tion [8–10]. This contribution is estimated by perform-

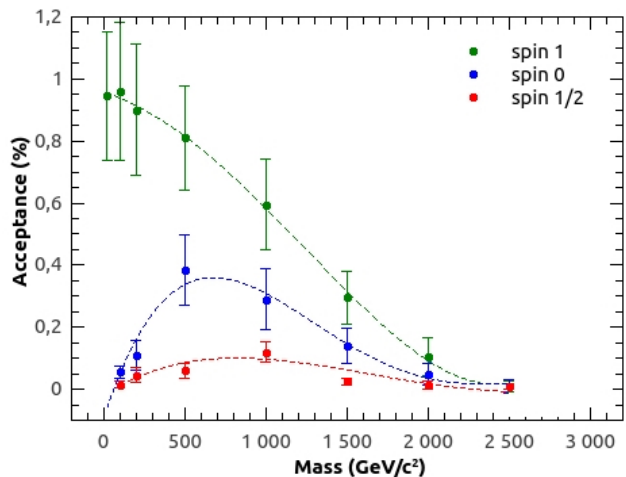


FIG. 10. Acceptance for spin-1, spin-0 and spin-1/2 HECOs with charge 125e.

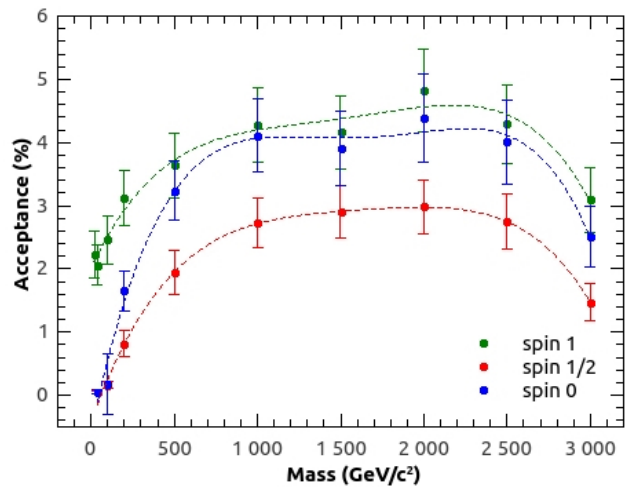


FIG. 11. Acceptance for monopole pair production with magnetic charge $2g_D$.

340 ing simulations with hypothetical material conservatively
 341 added and removed from the nominal geometry model.

342 An example, showing the MoEDAL NTD acceptance
 343 curves for spin-1/2, spin-0, spin-1 HECOs with charge
 344 125e is shown in Figure 10. The acceptance curves for
 345 spin-1/2 monopoles, found using the NTD and MMT de-
 346 tectors, are shown in Figure 11. The acceptances shown
 347 in Figure 10 and Figure 11 refer to the prototype detector
 348 deployed for LHC's Run-1.

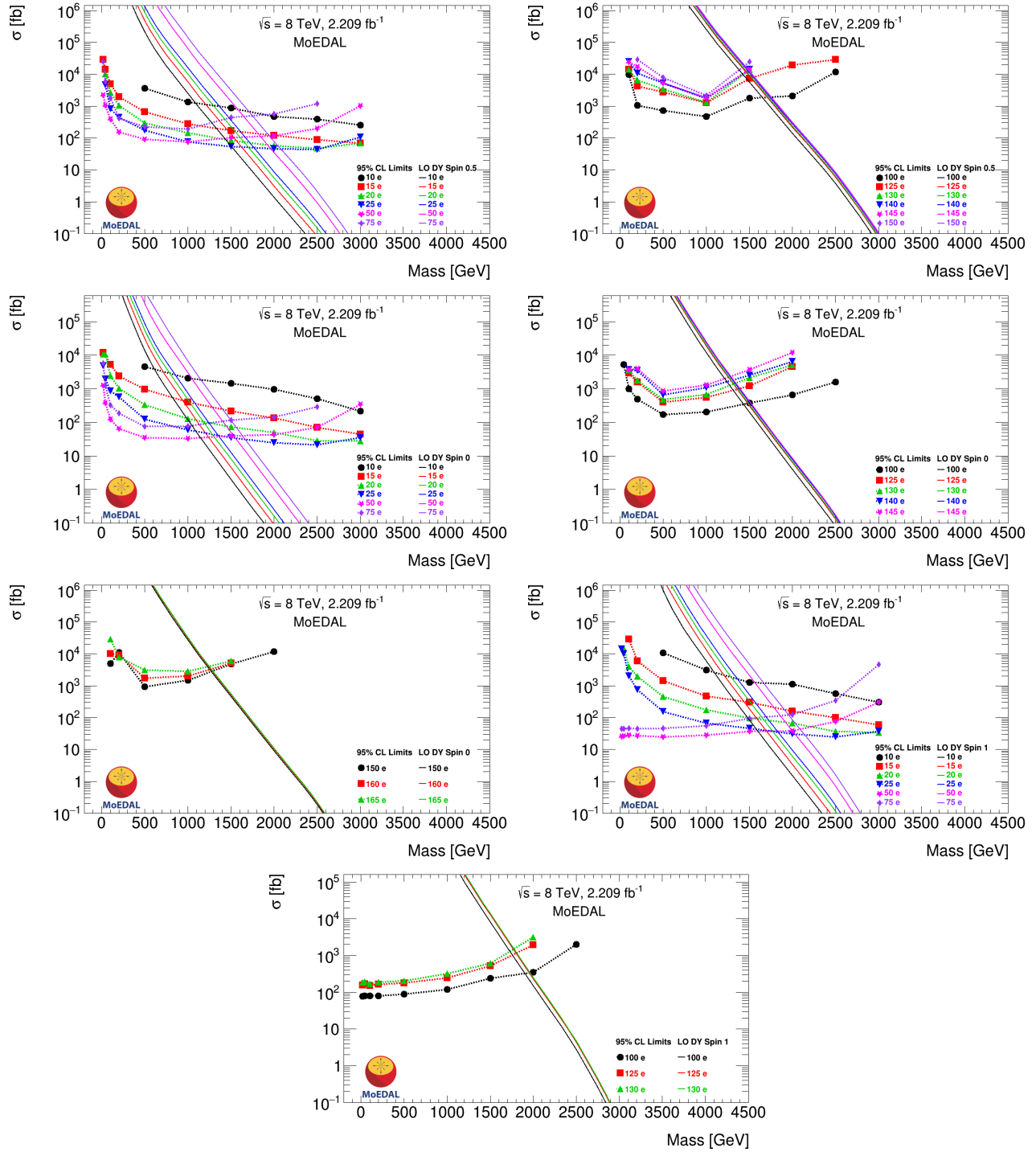
349

ANALYSIS RESULTS

350 The first Makrofol sheet of each of MoEDAL's 135
 351 NTD modules was etched and scanned, as described

TABLE I. Etching Conditions of Makrofol

Etching Mode	Etchant	v_B ($\mu\text{m}/\text{hour}$)
Strong	6N KOH + 20% ethyl alcohol at 65°C	23 ± 0.5
Soft	6N KOH + 20% ethyl alcohol at 50°C	3.4 ± 0.05

FIG. 12. 95% CL mass limits in a DY production model of spin-0, spin- $1/2$ and spin-1 HECO pair direct production in LHC pp collisions.

352 above, for evidence of the passage through the sheet of 353 a highly ionizing object such as a HECO or a magnetic

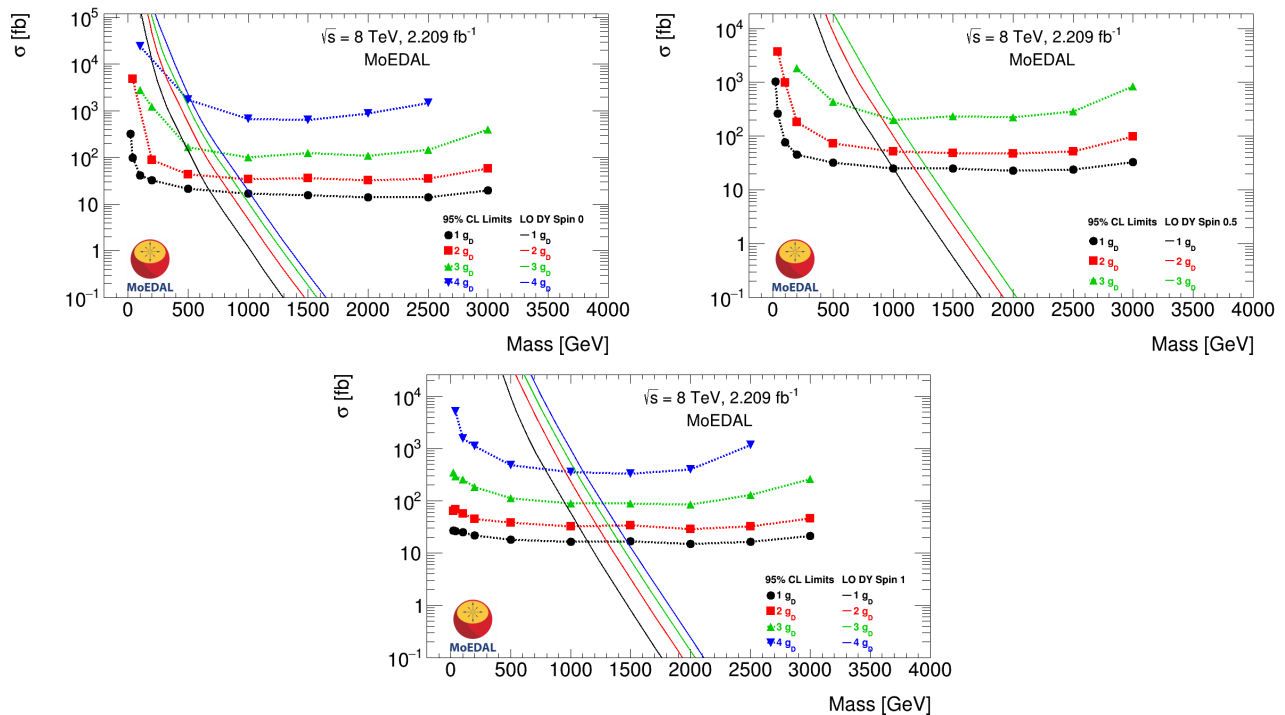


FIG. 13. 95% CL mass limits in a DY production model of spin-0, spin-1/2 and spin-1 monopole pair direct production in LHC pp collisions.

354 monopole. The total area of plastic analyzed was 7.8 m^2 .
 355 No candidate events were observed.

356 The material budget preceding the MoEDAL NTD
 357 modules is due to the presence of LHCb's VELO detector.
 358 It amounts to between 0.1 and 8.0 radiation lengths
 359 X_0 of material with an average of approximately $1.4 X_0$
 360 [42]. The dominant contribution to the systematic un-
 361 certainties in this analysis arises from the estimate of the
 362 material in the GEANT4 geometry description, resulting
 363 in a relative uncertainty of $\sim 10\%$ for a single charged
 364 monopole [8]. This uncertainty increases with electric
 365 and magnetic charge.

366 We calculated the 95% C.L. upper limits to the
 367 cross-section using as a measure a Drell-Yan model
 368 for HECO and magnetic monopole production assum-
 369 ing a β -independent monopole coupling and that the
 370 monopole can have a spin of 0, 1/2 and 1. The limit
 371 curves obtained are shown in Figure 12. For HECOs the
 372 cross section upper limits versus mass are given in Fig-
 373 ure 13 for spin 0, 1/2 and 1. The values of the limits are
 374 listed in Table II and Table III, for HECOs and magnetic
 375 monopoles, respectively.

CONCLUSIONS

377 Both MoEDAL's NTD system and aluminium ele-
 378 ments of the MoEDAL MMT detector were exposed to

379 8 TeV LHC collisions during Run-1 of the LHC. At the
 380 end of Run-1 both detector systems were examined for
 381 the presence of magnetic monopoles and/or HECOs. In
 382 the case of the MMT a SQUID-based magnetometer was
 383 utilized to search for the presence of trapped magnetic
 384 charge; the results were published in [8].

385 The NTDs were etched and scanned to reveal evidence
 386 for the passage of a magnetic monopole or a HECO using
 387 semi-automatic and manual optical microscopes.

388 In the final analysis no candidates for magnetic
 389 monopoles were found. Consequently, limits on the DY
 390 production of magnetic monopole pair with cross-section
 391 in the range of approximately 20 fb to 30 pb were set
 392 for magnetic charges up to $5g_D$ and mass as high as 1.2
 393 TeV. Additionally, no evidence was found for DY pro-
 394 duced HECO pairs. Thus, limits were placed on the DY
 395 production of HECO pairs with cross-sections from 20 fb
 396 to 30 pb, for electric charges as much as $165e$ and mass
 397 up to 2 TeV. The limits on the DY production of HECOs
 398 are the strongest to date at a collider experiment [15].

ACKNOWLEDGMENTS

400 We thank CERN for the LHC's successful Run-2 op-
 401 eration, as well as the support staff from our institu-
 402 tions without whom MoEDAL could not be operated.
 403 We acknowledge the invaluable assistance of particu-

TABLE II. 95% CL mass limits for the HECO search.

	Electric charge/e														
	10	15	20	25	50	75	100	125	130	140	145	150	160	165	
Spin	95% CL mass limits [GeV]														
0	640	950	1190	1350	1530	1500	1430	1360	1330	1310	1290	1280	1270	1260	
1/2	1090	1450	1650	1770	1840	1750	1650	1520	1470	1480	1490	1450	-	-	
1	1100	1440	1670	1840	2000	1960	1900	1800	1780	-	-	-	-	-	

TABLE III. 95% CL mass limits for the magnetic monopole search.

	magnetic charge/ g_D				
	1	2	3	4	5
Spin	95% CL mass limits [GeV]				
0	710	780	740	530	-
1/2	990	1090	1020	-	-
1	1150	1230	1210	1120	950

lar members of the LHCb Collaboration: G. Wilkinson, R. Lindner, E. Thomas and G. Corti. Computing support was provided by the GridPP Collaboration, in particular by the Queen Mary University of London and Liverpool grid sites. This work was supported by grant PP00P2_150583 of the Swiss NSF; by the UK Science and Technology Facilities Council, via the grants, ST/L000326/1, ST/L00044X/1, ST/N00101X/1 and ST/P000258/1; by the Generalitat Valenciana via a special grant for MoEDAL and via the projects PROMETEO-II/2017/033 and PROMETEO/2019/087; by MCIU / AEI / FEDER, UE via the grants FPA2016-77177-C2-1-P, FPA2017-85985-P, FPA2017-84543-P and PGC2018-094856-B-I00; by the Physics Department of King's College London; by NSERC via a project grant; by the V-P Research of the University of Alberta (UofA); by the Provost of the UofA); by UEFISCDI (Romania); by the INFN (Italy); by the Estonian Research Council via a Mobilitas Plus grant MOBTT5; and by a National Science Foundation grant (US) to the University of Alabama MoEDAL group.

- [1] M. Fairbairn et al., Stable Massive Particles at Colliders, Phys. Rept. 438 (2007).
- [2] L. Patrizzii and M. Spurio, Status of Searches for Magnetic Monopoles, Annu. Rev. Nucl. Part. Sci. 65, 279 (2015)
- [3] B. Acharya et al., MoEDAL Collaboration, Physics Programme Of The MoEDAL Experiment At The LHC, Int. J. Mod. Phys. A29, 1430050 (2014).
- [4] G. Aad et al., ATLAS Collaboration, Search for massive long-lived highly ionizing particles with the ATLAS detector at the LHC, Phys. Lett. B 698, 53 (2011).
- [5] G. Aad et al., ATLAS Collaboration, Search for Magnetic Monopoles in $\sqrt{s} = 7$ TeV pp Collisions with the ATLAS Detector, Phys. Rev. Lett. 109, 261803 (2012),
- [6] G. Aad et al., ATLAS Collaboration, Search for long-lived, multi-charged particles in pp collisions at $\sqrt{s} = 7$ TeV using the ATLAS detector, Phys. Lett. B 722, 305 (2013).
- [7] G. Aad et al, ATLAS Collaboration, Search for magnetic monopoles and stable particles with high electric charges in 8 TeV pp collisions with the ATLAS detector, Phys. Rev. D 93, 052009 (2016).
- [8] B. Acharya et al., MoEDAL Collaboration, Search for magnetic monopoles with the MoEDAL prototype trapping detector in 8 TeV proton-proton collisions at the LHC, JHEP 08, 067 (2016).
- [9] B. Acharya et al., MoEDAL Collaboration, Search for magnetic monopoles with the MoEDAL forward trapping detector in 13 TeV proton-proton collisions at the LHC, Phys. Rev. Lett. 118, 061801 (2017).
- [10] B. Acharya et al., MoEDAL Collaboration, Search for magnetic monopoles with the MoEDAL forward trapping detector in 2.11 fb⁻¹ of 13 TeV proton-proton collisions at the LHC, Phys. Lett. B 782, 510 (2018).
- [11] B. Acharya et al., MoEDAL Collaboration, Magnetic Monopole Search with the Full MoEDAL Trapping Detector in 13 TeV pp Collisions Interpreted in Photon-Fusion and Drell-Yan Production, Phys.Rev.Lett. 123, 021802 (2019).

* Also at Int. Centre for Theoretical Physics, Trieste, Italy
† Also at National Institute of Chemical Physics & Biophysics, Tallinn, Estonia
‡ Also at Dept. of Physics, Faculty of Science, Beni-Suef University, Egypt
§ Now deceased
¶ Also at Physics Department, University of Regina, Regina, Saskatchewan, Canada
** Corresponding author: jpinfold@ualberta.ca
†† Also at Centre for Astronomy, Astrophysics and Geophysics, Algiers, Algeria

- 474 [12] ATLAS Collaboration, Search for heavy long-lived multi-
475 charged particles in pp collisions at $\sqrt{s} = 8$ TeV using
476 the ATLAS detector, *Eur. Phys. J. C* 75, 362 (2015).
- 477 [13] S. Chatrchyan et al., CMS Collaboration, Searches for
478 long-lived charged particles in pp collisions at $\sqrt{s} = 7$
479 and 8 TeV, *JHEP* 07, 122 (2013) 122.
- 480 [14] M. Aaboud, ATLAS Collaboration, Search for heavy
481 long-lived multi-charged particles in proton-proton col-
482 lisions at $\sqrt{s} = 13$ TeV using the ATLAS detector, *Phys.*
483 *Rev. D* 99, 052003 (2018) 052003.
- 484 [15] G. Aad et al., The ATLAS Collaboration, Search for
485 Magnetic Monopoles and Stable High-Electric Charged
486 Objects in 13 TeV Proton-Proton Collisions with the AT-
487 LAS Detector, *Phys. Rev. Lett.*, 124, 3 031802 (2020).
- 488 [16] S. Burdin et al., Non-collider searches for stable massive
489 particles, *Phys. Rept.* 582, 1(2015).
- 490 [17] L. Patrizzii, Z. Sahnoun, and V. Togo, Searches for cos-
491 mic magnetic monopoles: past, present and future, *Phil.*
492 *Trans. R. Soc. A* 377: 20180328 (2019).
- 493 [18] J. Beringer et al. (Particle Data Group), *Phys. Rev. D* 86,
494 0100001 (2012).
- 495 [19] P. A. M. Dirac, Quantised Singularities in the Electro-
496 magnetic Field, *Proc. Roy. Soc. A* 133, 60 (1931).
- 497 [20] G. 't Hooft, Magnetic Monopoles in Unified Gauge The-
498 ories, *Nucl. Phys. B* 79, 276 (1974).
- 499 [21] A. M. Polyakov, Particle Spectrum in the Quantum Field
500 Theory, *JETP Lett.* 20, 194 (1974).
- 501 [22] H. Georgi and S. Glashow, Unified weak and electromag-
502 netic interactions without neutral currents. *Phys. Rev.*
503 *Lett.*, 28, 1494 (1972).
- 504 [23] H. Georgi and S. Glashow, S. Unity of all elementary
505 particle forces. *Phys. Rev. Lett.*, 32, 438–441 (1974).
- 506 [24] Y.M. Cho and D. Maison, *Phys. Lett. B* 391, 360 (1997).
- 507 [25] W.S. Bae and Y.M. Cho, *JKPS* 46, 791 (2005).
- 508 [26] Y. M. Cho, K. Kim and J. H. Yoon, *Eur. Phys. J. C* 75,
509 no. 2, 67 (2015).
- 510 [27] J. Schwinger, A Magnetic Model of Matter. *Science.* 165,
511 757-761 (3895).
- 512 [28] J. Ellis, N. E. Mavromatos, T. You, The Price of an
513 Electroweak Monopole, *Phys. Lett. B* 756, 20-35 (2016).
- 514 [29] B. Holdom, J. Ren, and C. Zhang, Quark Matter May
515 Not Be Strange, *Phys. Rev. Lett.* 120, 222001 (2018).
- 516 [30] E. Farhi and R. Jaffe, Strange matter, *Phys. Rev. D* 30,
517 2379 (1984).
- 518 [31] S. Coleman, Q-balls, *Nucl. Phys. B* 262, 263 (1985).
- 519 [32] A. Kusenko and M. E. Shaposhnikov, Supersymmetric
520 Q-balls as dark matter, *Phys. Lett. B* 418(1998) 46.
- 521 [33] B. Koch, M. Bleicher, and H. Stöcker, Black holes at
522 LHC? *J. Phys. G* 34 S535 (2007).
- 523 [34] E. V Benton and W. D. Nix, The restricted energy loss
524 criterion for registration of charged particles in plastics,
525 *NIM* 67, 343-347 (1969).
- 526 [35] L.P. Gamberg, G.R. Kalbfleisch and K.A. Milton, Direct
527 and indirect searches for low mass magnetic monopoles,
528 *Found. Phys.* 30, 543 (2000) 543.
- 529 [36] C.J. Goebel, Binding of nuclei to monopoles, in *Monopole*
530 *'83*, J.L. Stone ed., Plenum(1984), p. 333.
- 531 [37] L. Bracci and G. Fiorentini, Interactions of Magnetic
532 Monopoles With Nuclei and Atoms, *Nucl. Phys. B* 232,
533 236 (1984).
- 534 [38] K. Olausen and R. Sollie, Form-factor effects on
535 nucleus-magnetic monopole binding, *Nucl. Phys. B* 255,
536 465 (1985).
- 537 [39] A. De Roeck et al., Development of a magnetometer-
538 based search strategy for stopped monopoles at the Large
539 Hadron Collider, *Eur. Phys. J. C* 72, 2212 (2012).
- 540 [40] S. Balestra et al., Magnetic monopole search at high al-
541 titude with the SLIM experiment, *Eur. Phys. J. C* 55,
542 57–63 (2008).
- 543 [41] S. Balestra et al., Bulk etch rate measurements and cal-
544 ibrations of plastic nuclear track detectors, *NIM-B* 254,
545 254-258 (2007).
- 546 [42] A. A. Alves Jr., et al., LHCb Collaboration, The LHCb
547 Detector at the LHC, *JINST* 3, S08005 (2008).
- 548 [43] L.A. Harland-Lang, V.A. Khoze, M.G. Ryskin “Ex-
549 clusive LHC physics with heavy ions: SuperChic 3”
550 arXiv:1810.06567
- 551 [44] P.J.W. Faulkner et al., GridPP: development of the UK
552 computing Grid for particle physics, *Journal of Physics*
553 *G: Nuclear and Particle Physics*, 32(1), N1-N20 (2006)
- 554 [45] D. Britton et al., GridPP: The UK grid for particle
555 physics, *Phil. Trans. R. Soc.* 367(1897):2447-57 (2009)